

MODULER SNAKE ROBOT

Project Report

Robotics Club

Designed by

Robotics Core Members

2023-2024

Under the guidance of

G.Praveen Kumar



Accredited by NBA

Geethanjali College of Engineering and Technology

(UGC Autonomous)

(Affiliated to J.N.T.U.H, Approved by AICTE, New Delhi)

Cheeryal (V), Keesara (M), Medchal. Dist.-501 301.

December-2023

Table of Contents

- 1) Abstract
- 2) Mechanical Design
 - a) Design inspiration
 - b) Materials Used
 - c) Kinematics Model
 - d) Dynamics Model
 - e) Lateral Undulation
 - f) Sidewinding Locomotion
- 3) Electronics
 - a) Components Used
 - b) Circuit Diagrams
- 4) Source Code
 - a) Software Used
 - b) Libraries Used
 - c) Brief Explanation
- 5) Conclusion
- 6) Bibliography

Abstract

Robots that aim to reproduce serpentine motion have been a subject of interest among engineers for a very long period of time due to several reasons. Snakes achieve a much higher degree of flexibility and adaptability to their immediate terrain than organisms that use limbs for locomotion while maintaining the same level of efficiency. Thus, building robots that can emulate the gaits displayed by snakes can enable us to access difficult-to-reach areas and harsh terrain with minimal power cost.

This project aims to create a snake robot that emulates a few of the gaits that snakes use, namely lateral undulation and sidewinding locomotion in a modular, compact, low-power and relatively low cost manner. As a result, the snake can maneuver over several slippery surfaces through the use of sidewinding locomotion, while maintaining high speed travel using lateral undulation.

This hybrid of both gaits allows us to combine the best of both worlds, meaning the robot can move at a high speed when using lateral undulation and shift to sidewinding locomotion when difficult terrain has to be navigated. Such a bot has a myriad of applications, including but not limited to search and rescue operations, stealth operations and wildlife research.

Mechanical Design

Our snake robot used the partitioned gait template (Fig. a) from our recent animal observations [24]. The robot is 823.3 mm long, 70 mm breadth and 68 mm height and weighed 2.75kg excluding off-board controllers. To enable large body deformation both laterally and dorsoventrally for traversing large steps (and complex three-dimensional terrain in general), the robot consists of 12 segments with 10 servo-motors connected by alternating pitch and yaw joints. We refer to segments containing pitch or yaw joint servo-motors as pitch or yaw segments, respectively. An anisotropic friction profile, with smaller forward friction than backward and lateral friction, is critical to snakes' ability to move on flat surfaces using lateral undulation [25]. To achieve this in the robot, we added to each pitch segment a pair of one-way wheels (12 mm diameter, with a rubber O-ring on each wheel) realized by a ratchet mechanism similar to [26]. The one-way wheels unlocked when rotating forward and locked when rotating backward, resulting in a small forward rolling friction and a large backward sliding friction, besides a large lateral sliding friction. We measured the kinetic friction coefficient at various body orientations and confirmed that forward friction was indeed smaller than backward and lateral friction (Fig. b).

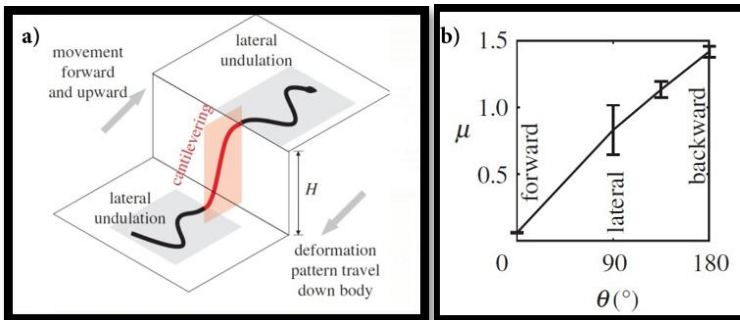


Fig. a Fig. b

Fig 0: Gait and mechanical design of snake robot. (a) Partitioned gait template from kingsnakes combining lateral undulation and cantilevering to traverse a large step [26]. Lateral undulation can be simply controlled and varied using a few wave parameters, such as wavelength, amplitude and frequency. Three segments are dragged by a weight using a string through a pulley with various orientation angle θ between body long axis and direction of drag force. $\theta = 0^\circ$, 90° and 180° are for sliding in body's forward, lateral and backward directions, respectively. Arrow on one-way wheel shows its direction of free rotation. (b) Kinetic friction coefficient as a function of body orientation θ .

Design Inspiration

Snake robots are hyper-redundant mechanisms [1] that consist of a large number of actuated links chained together in series. Their many degrees of freedom give them the potential to navigate a wide range of environments. The history of snake robot's dates back to Shigeo Hirose's pioneering work with the Active Cord Mechanism (ACM) [2], shown in Fig. 1. Since then, Hirose as well as others in Japan have developed additional generations of snake robots that are adept at a wide range of tasks [3,4].



Fig. 1: The Unified Snake robot (left) and one of the individual 1-DOF modules from the snake robot (right).

Many of these snake robots utilize passive wheels, like the screw drive mechanism of Hara et al. [5] or the passive-wheeled snake by Kamegawa et al. that can climb pipes and poles [6]. The group at Carnegie Mellon has developed modular snake robots that rely solely on their internal shape changes to locomote through their environment [7, 8]. In many ways the design and architecture of our robot draws from the field of reconfigurable modular robots like Yim's PolyBot [9,10].

Approaches to controlling articulated snake robots often rely on cyclic motions, gaits, based on the modal backbone curves [11, 12, 13] or follow-the-leader controllers [14, 15, 16]. A bio-inspired approach to control includes the use of central pattern generators (CPGs). Gonzalez-Gomez et al. [17] use CPGs to control a modular robot of different topologies and Ijspeert et al. [18] control the swimming motion of a snake-like robot. This approach of using lower-dimensional cyclic controllers and controlling the robot in a strongly feed forward manner forms the basis of our approach to locomotion, [19]. Overall, the approach has been to command the shape of the robot directly and low-pass the controller parameters to maintain smooth motion, as opposed to CPGs that use a tuned network of neural oscillators to

generate a limit cycle of the robot's shape. We were inspired to begin this project after seeing research videos of both tree climbing robotic snakes and robotic eels.

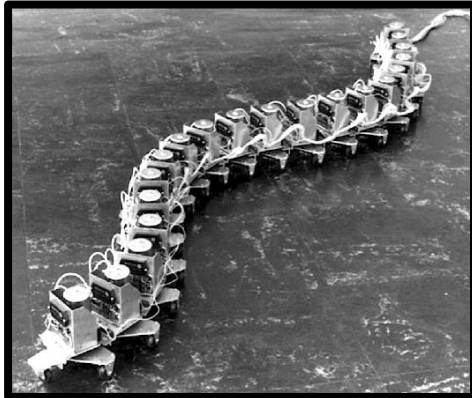


Fig. 2: One of Hirose's early Active Cord Mechanisms (ACM-III).

Other important work includes Chirkjian and Burdick, who consider both the locomotion [20] and manipulation [21] aspects of hyper redundant mechanisms. Their approaches specify modes and shape functions that are chosen based on full knowledge of both the robot's configuration and its environment. Transeth et al. have developed a robot and control framework capable of obstacle-aided locomotion [22]. While their robot has the ability to sense and adapt their motions to obstacles, it is restricted to planar motions in a lab-controlled environment. A thorough survey of snake robot modeling and locomotion is provided by Transeth and Pettersen [23].

Design Process

3D model printing technology is used in the iterative design of the snake robot. It can reduce the design cycle and cost. Ultimately, the snake robot's shell and body use PETG (Polyethylene Terephthalate Glycol) to maintain the structural strength and decrease the overall weight of the snake robot to improve its movement flexibility. The robot parts all use socket head cap screw fasteners, which is convenient for disassembly. The internal circuit and battery of the joint are fixed on the Servo Mount frame to ensure its shake-resistance and stability. In each of the joints of the external structure, an "Hardy-Lock Type Mechanism" is used to prevent water and other debris from entering the robot. The snake robot's head is a specially designed scratch-resistant plastic compound. It improves the robot's environmental compatibility, providing features such as anti-scratch and wear-resistance abilities, which do not decrease the camera transmission efficiency and maintains acceptable distortion. The final installed and integrated snake robot is shown in Figure 17.

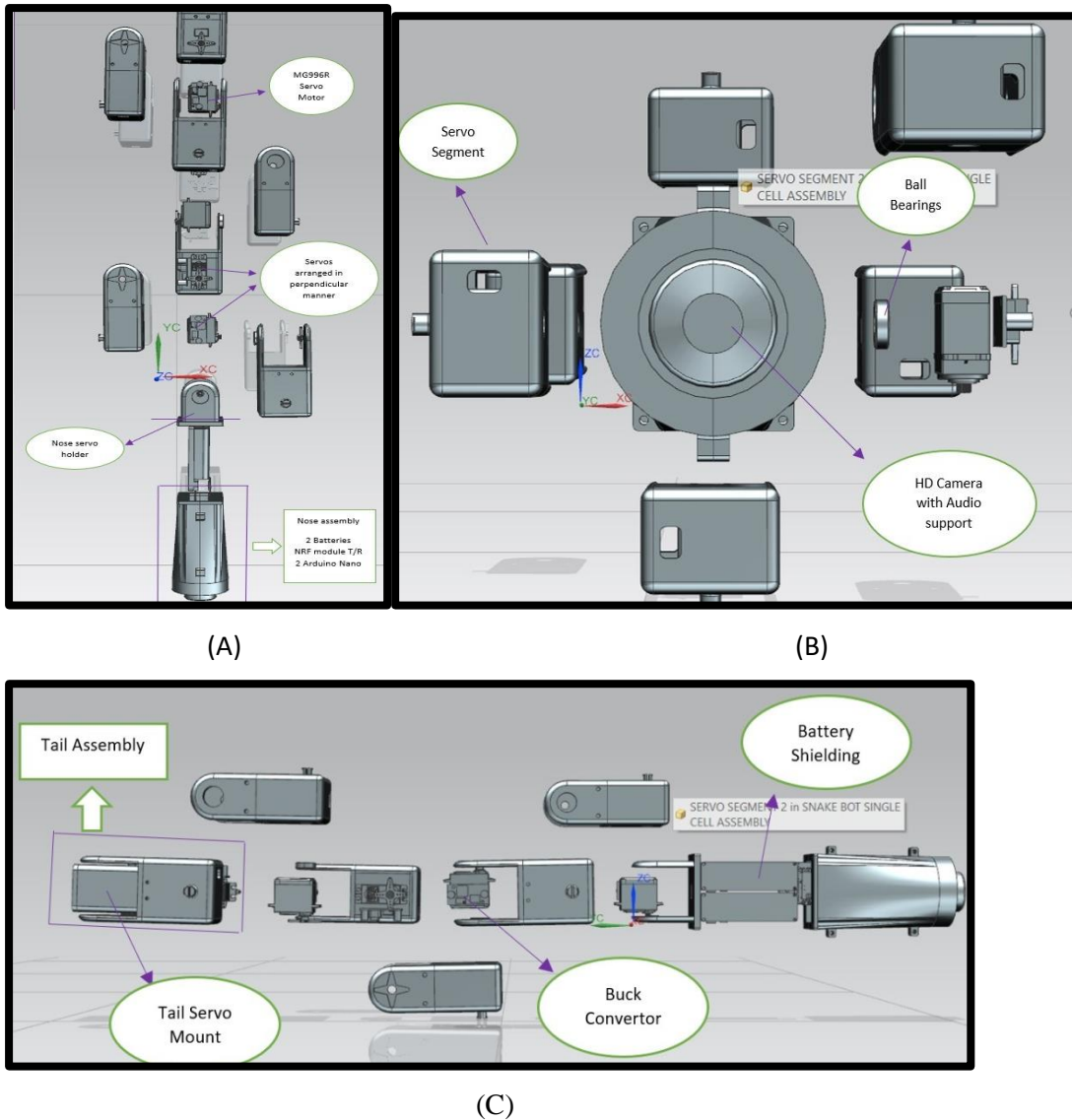


Fig. 17: (a) Top View, (b) Front View, (c) Right-Side Views are the “3rd Angle Isometric 3D projections” done in **NX CAD & SOLIDWORKS 2021**.

Materials Used

Since space and weight are extremely constrained in our snake robot, the material choice is important. The specific energy of various materials in terms of both mass and volume are to be chosen specifically from Additive Manufacturing. Due to certain testing of thermoplastic materials the data of PLA (Polylactic Acid); ABS (Acrylonitrile butadiene styrene); PETG (Polyethylene Terephthalate Glycol) has been represented here in Table 1. And by that we looked for a polymer which is more reliable and can withstand the environment and consequently must cope with harsh situations. We mean that Glass transition temperature must be stable and constant as well as the specific heat capacity of the total model after testing without any loose ends (or) overhangs. Also, the constant radiation and convection of

the robot components must be compact the overall design, So the PETG was a good idea to use when exposed to sunlight and environment being a polyethylene group that has its special property to adhere to its compactness.

Material	Specific Heat Capacity (J/kg-K)	Glass Transition Temperature (°C)
PLA	1800	60
ABS	2200	105
PETG	2400	85

Table. 1: Both Weight and volume of the [PETG] has by far the greatest performance.

Design Parts

The Snake bot consists of initial components like:

- i. Head
- ii. Servo Modules
- iii. Servo Connectors
- iv. Tail.

- **Head:** In the Snake Head as per the components required to place in them there would be Wi-Fi Camera (V380) (1), Arduino Nano (1), 18650 Battery Shield (2), 18650 Batteries 2000mah (2) clearly labelled in Fig. 3

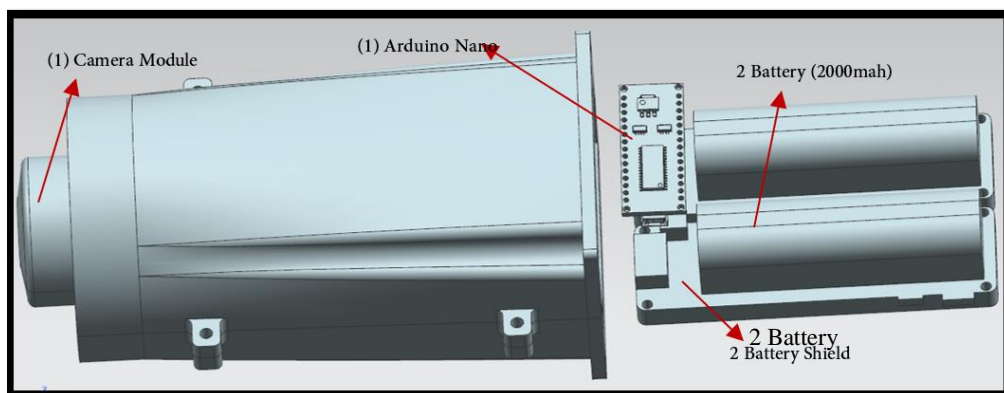


Fig. 3: Exploded View of Head Module Assembly.

- **Servo Modules:** It consists of snake 3.7V/1950mah (2) batteries in series, Servo Motor MG996R (1), Buck Converter (LM2596) (1) and these are connected in orderly fashion to nose servo mount near to head. Our snake bot has 10 modules connected in perpendicular order and by increasing them the snake motion and actuation may vary accordingly. As shown in Fig. 4 & Fig. 5

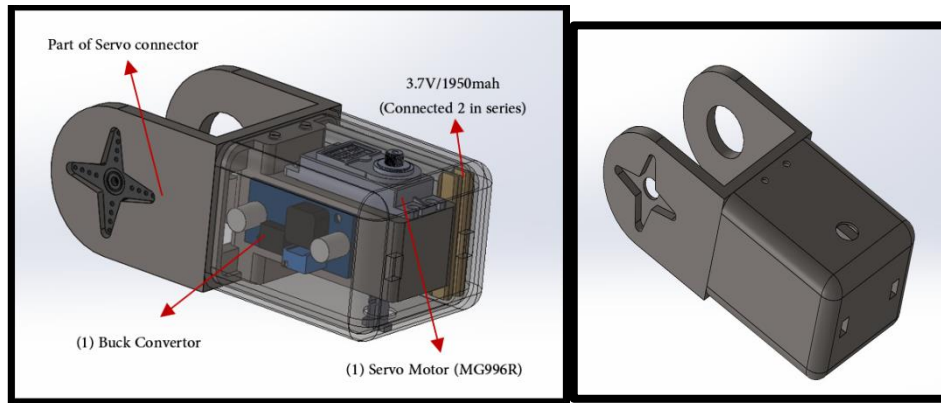


Fig. 4: Exploded View of Servo Module Assembly.

Fig. 5: Isometric View of Servo Module Assembly.

- **Servo Connectors:** These are the fixtures (or) slots of servo motors in which they hold a buck converter, 3.7V/1950mah Batteries and usually the Servo motor (MG996R). And they directly fit in the servo modules respectively as shown in the Fig. 4

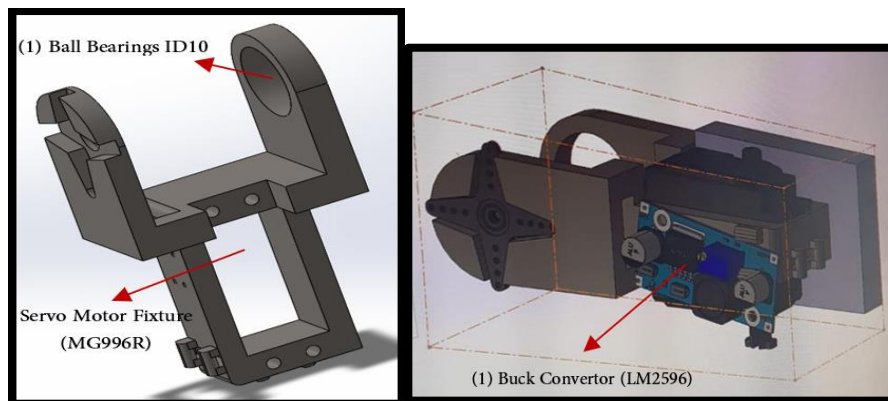


Fig. 6: Rendered design of Servo Connector **Fig. 7:** Bounding Box of Servo Connector

We designed them specifically for compactness of the environment and therefore, it can hold the required components by suitable dimensions.

- **Tail:** It consists of a tail servo connector which is again redesigned to fill its space to connect the other modules and to complete the links of the snake robot in a manner. The Tail cap will be connected to the tail servo connector as shown in Fig. 8 & Fig. 9



Fig. 8: 3D-Printed parts of Tail Cap

Fig. 9: 3D-Printed parts of Tail Servo Connector

Kinematics Model

In order to design a snake robot that utilizes a concertina gait, it would be advantageous to have a kinematics and dynamics model for a multi-linked snake robot that is moving in such a fashion [27] [28]. By being able to compute the torque as a function of time during the entire course of motion for the gait, relevant information about the snake robot design (metrics such as effort) can be [29] extracted. In order to develop functional modular snake robots, they must be designed to optimize certain functional requirements and performance characteristics.

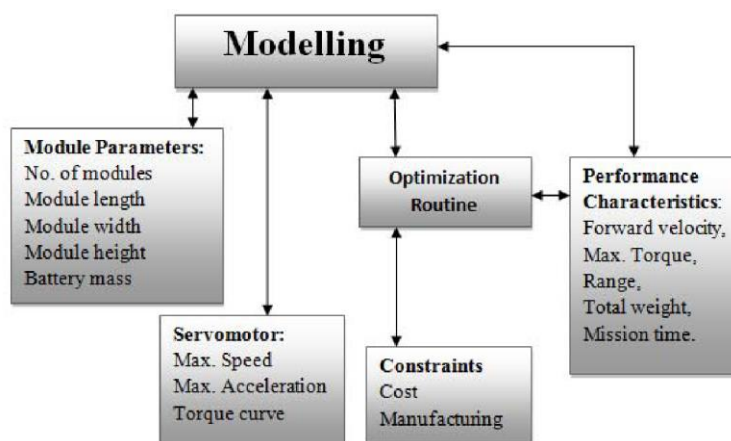


Fig.10: Detailed Flowchart for Modelling a Snake Robot.

The Strategy of the Head Control

The strategy of the head control is segmented, and it is divided into the calculations of the joint angles for the base part, the neck part and head part. The joint angles of the base part are obtained by discretizing the backbone curve of the base part. For the neck part, the desired pose for the head link and the dexterous workspace of the head part can in turn derive a desired position and direction of the end frame of the neck part. The joint angles are determined by making the end frame of the neck part approach the desired one. Thus, the dexterous workspace and the centre of the dexterous workspace of the head part are needed. Once the neck part is determined, the end frame of the neck part is used for the base frame of the head part. The joint angles of the head part can be solved by the inverse kinematics algorithm.

1.1. The Calculation of Joint Angles for the Base Part

The axis of the snake robot is orthogonal to each other and the joint has only one degree of freedom. This structure is widely adopted by the researcher in the snake robot field [30,31,32]. The robot has two types of joints, the yaw joint and the pitch joint. The illustration of the snake robot configuration can be seen in Fig.11a. This configuration can help the snake robot to achieve motion in three-dimensional space. The base part of the robot is the part contacting with the ground Fig 11b.

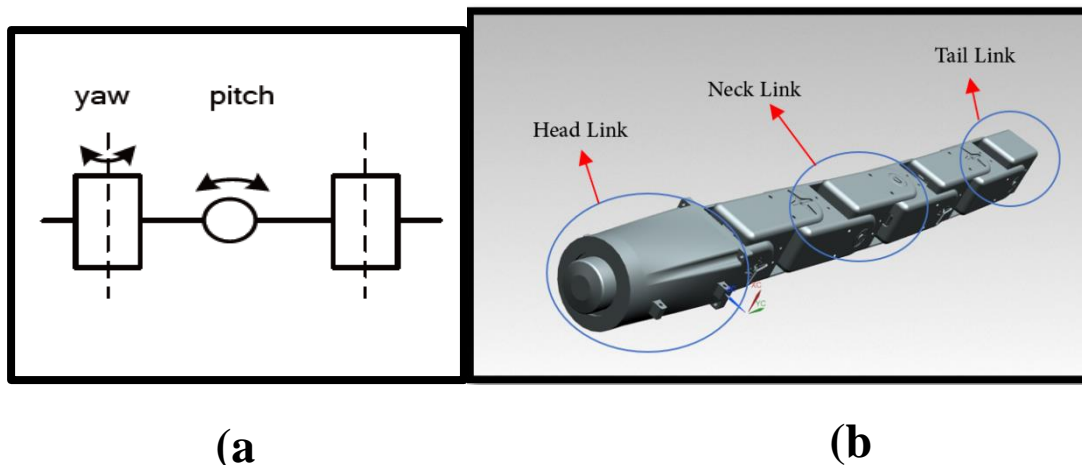


Fig. 11: (a) The axis of each joint is rotated 90 degrees relative to the previous joint axis; yaw joint generates rotation out of the plane, while pitch joint generates rotation in the plane in this illustration. (b) The overview of the snake robot.

In the process of the head control for the snake robot, the base part is used to ensure the body of the snake robot keeps stable. The support polygon method and zero-moment point method are usually used to judge whether the body is stable [33]. When the support polygon has a

larger area, the body will have a greater possibility of stable standing. As we know, for a given perimeter of the polygon, the circle has the largest coverage area among all the plane polygons. Thus, we design the backbone of the base part as a plane circle. Then we use the backbone curve theory to discretize the backbone curve to generate the joint angles of the base part. The support polygon and the backbone curve is shown in Figure 12.

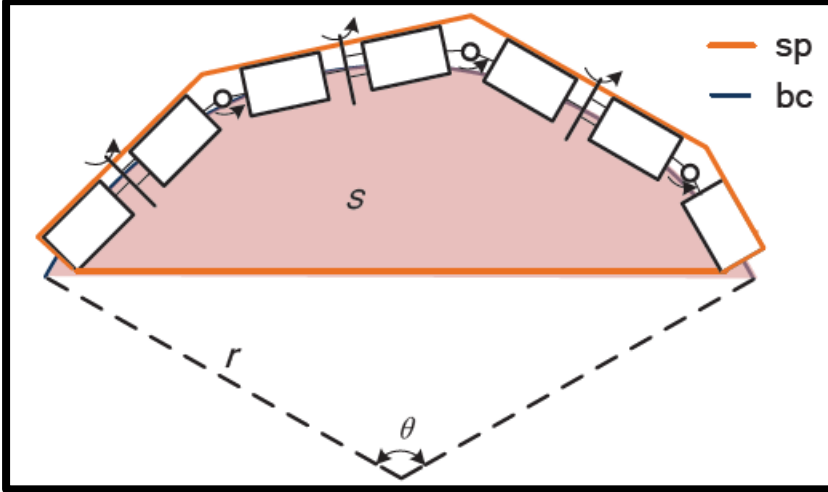


Fig.12: The support polygon constructed by the base part of the snake robot and the plane arc backbone curve. The symbol 'bc' means backbone curve and symbol 'sp' means support polygon.

We assume that the backbone curve of the base part has a length l , and the joint angles of the base part are generated by discretizing a plane arc with a radius r . Thus, we have the following equations,

$$r = \frac{l}{\theta} \quad (1)$$

$$S = \frac{1}{2}r^2(\theta - \sin(\theta)) \quad (2)$$

where θ is the central angle of the plane arc, and S is the area enclosed by the backbone curve, shown

in Figure 12. When θ equals π , S have the maximum value $1/2\pi r^2$. More details about the support

polygon and zero-moment point will be introduced in Section 3. After the backbone curve of the base part is determined, we need to discretize the backbone curve to obtain joint angles. We adopt the discretization method based on the curvature and torsion of the backbone curve [34]. The corresponding formulas are given as:

$$\phi = \int_0^s \tau(s) ds \quad (3)$$

$$\begin{cases} \kappa_y(s) = \kappa(s) \cos(\phi) \\ \kappa_p(s) = \kappa(s) \sin(\phi) \end{cases} \quad (4)$$

$$\theta_y = \int_{s_1}^{s_2} \kappa_y(s) ds \quad (5)$$

$$\theta_p = \int_{s_1}^{s_2} \kappa_p(s) ds \quad (6)$$

where $k(s)$ and $t(s)$ are the curvature and the torsion of the backbone curve at the arc length s . ϕ is the phase angle of the discretization. In addition, it is obtained by the integral of the torsion on the arc length s . In addition, it describes the twist of the Frenet–Serret frame along the backbone curve [35]. κ_y and κ_p are the curvature projection on the yaw direction and the pitch direction, which are used to describe the bending along the yaw and pitch direction. Furthermore, θ_y and θ_p are the yaw joint angles and the pitch joint angles of the base part shown in Figure 11a. s_2 and s_1 in Equations (5) and (6) are the start arc length and end arc length of the discretization respectively. For a spatial curve $\mathbf{r}(t)$, its curvature k and torsion t can be calculated as [35]:

$$\begin{cases} \kappa = \frac{|\mathbf{r}' \times \mathbf{r}''|}{|\mathbf{r}'|^3} \\ \tau = \frac{(\mathbf{r}' \times \mathbf{r}'') \cdot \mathbf{r}'''}{|\mathbf{r}' \times \mathbf{r}''|^2} \end{cases} \quad (7)$$

where \mathbf{r}' , \mathbf{r}'' and \mathbf{r}''' are the first, second and third order derivatives of \mathbf{r} to the general parameter

t , respectively. For the plane arc, it has the curvature $k = 1/r$ and torsion $t = 0$. In addition, Equations (4), (6) can be simplified to

$$\begin{cases} \kappa_y = \kappa(s) \\ \kappa_p = 0 \end{cases} \quad (8)$$

$$\begin{cases} \theta_y = \kappa_y \Delta s \\ \theta_p = 0 \end{cases} \quad (9)$$

where $\Delta s = s_2 - s_1$. In addition, substitute $k = 1/r$ into Equation (9), the result that $\theta_y = \frac{\Delta s}{r}$ is obtained. The discretization result of the plane arc is shown in Figure 3.

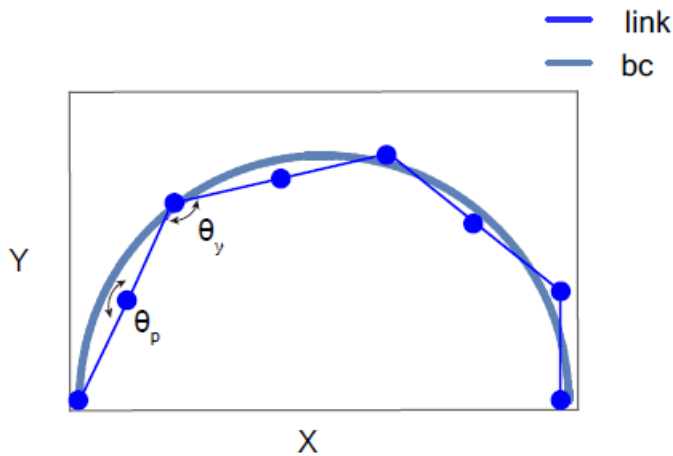


Fig.13: The discretization result of the plane arc backbone curve. The symbol 'bc' means backbone curve.

Dynamics Model

The snake robot can be modelled as a series of n rigid links, each of length and mass l_i and m_i . The distance from joint i to the centre of mass of link i is denoted l_{Gi} , and the distance to the friction contact point l_{fi} . Each link is connected with actuators that allow for the control of the relative angle at the joints between links. Each link can be subjected to three external forces, a gravitational force, frictional force, and constraint forces due to the other links.

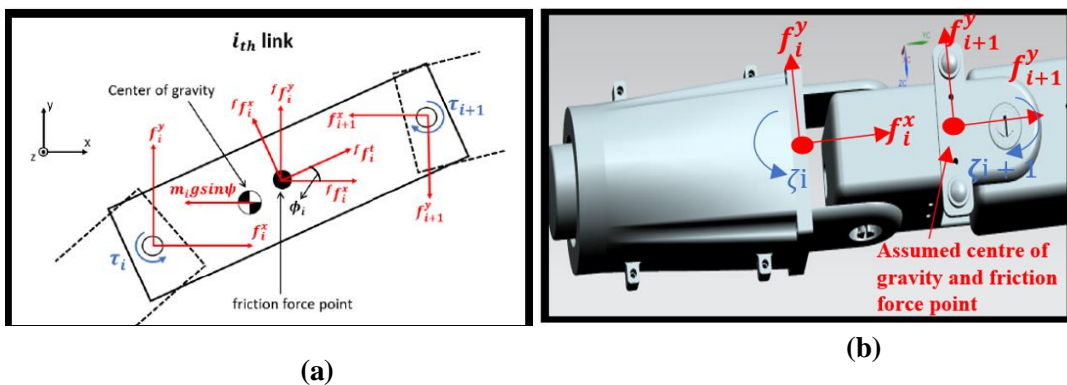


Fig. 14: Figure 14a (adapted from reference [40]) shows a schematic of the gravitational, frictional, and constraint forces acting on an individual link. The friction forces are assumed to be concentrated at a single point for convenience. Figure 14b shows where these forces are assumed to act on an actual link of our robot.

The anisotropic property of snake scales can be imitated using wheels underneath each link to allow rolling in the tangential direction, thus the friction force is assumed to be acting at a single point on each link, as shown in Figure 14a. The following models are developed in two dimensions in reference to an absolute inertial coordinate frame. For a robot moving on flat ground, the gravitational force $mg\sin\psi$ can be ignored.

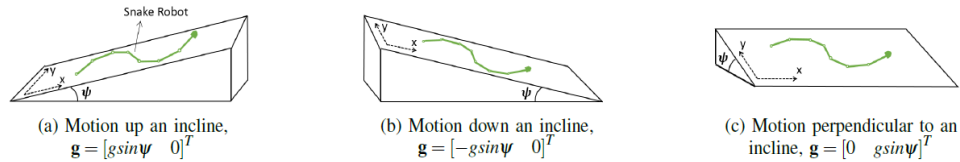


Fig. 15. Three different motion scenarios will be studied for an incline of degree ψ . Coordinate setup is shown for each scenario, where the definition of \mathbf{g} will depend on each scenario ($g = 9.8\text{N}$).

- **Serpentine Locomotion Modelling**

Hirose was one of the first to mathematically define the specific curve that a snake's body follows during lateral undulatory motion, proposing the "Serpenoid" curve [36], characterized by a sinusoidally varying curvature as a function of arc length. Ma developed a slightly different mathematical function he termed the "Serpentine" curve based on a physiological analysis of snake muscle contractions, purporting a higher locomotive efficiency and more realistic representation of lateral undulatory motion due to the consideration of snake's actual musculo-skeletal structure and muscular forces [36]. However the Serpentine curve is quite mathematically complex, thus for purposes of convenience in analysis and simulation, Ma uses the Serpenoid curve in his later work [37, 38] to analyze the dynamic equations and motion characteristics. In this discussion, the "Serpenoid" curve is defined by the following curvature function [37, 38]:

$$\kappa(s) = \frac{-2K_n\pi\alpha_0}{L} \sin\left(\frac{2K_n\pi}{L}s\right), \quad (1)$$

where L , α_0 , and K_n represent the total arc length, initial curve amplitude, and degree of the curve. For simplicity, in this paper $K_n = 1$ always. Assuming an initial position and orientation at the origin, the tangential angle along the curve can be derived by integrating the curvature function with respect to arc length:

$$\phi(s) = \int \kappa(s) ds = \alpha_0 \cos\left(\frac{2K_n\pi}{L}s\right) + \phi_{off}. \quad (2)$$

ϕ_{off} represents an offset angle that will rotate the curve about the azimuthal axis. This equation can be discretized to apply to a snake-robot consisting of n links, total length L , and link length of $L/n = l$. The relative joint angles can be derived by taking the difference of tangential angles at the centre of adjacent links:

$$\begin{aligned} \theta_i(s) &= \phi(s + il + l/2) - \phi(s + il - l/2) = \\ &= -2\alpha_0 \sin\left(\frac{K_n\pi}{n}\right) \sin\left(\frac{2K_n\pi}{L}(s + il)\right), \quad i = 1, \dots, n-1. \end{aligned} \quad (3)$$

The absolute angle measured from the x axis of each link is given by

$$\phi_{i+1} = \theta_{i+1} + \phi_i.$$

Applying this relation to an n -dimensional vector for all links, $\phi = [\phi_0 \dots \phi_{n-1}]^T$; yields the following relation:

$$\phi = E\theta + e\phi_0, \quad (4)$$

where

$$\begin{aligned} \mathbf{e} &= [1 \dots 1]^T \in \mathfrak{R}^n, \\ \mathbf{E} = \{E_{(i,j)}\} &\in \mathfrak{R}^{n \times (n-1)}, \quad E_{(i,j)} = \begin{cases} 1 & i > j, i > 1 \\ 0 & \text{otherwise,} \end{cases} \end{aligned}$$

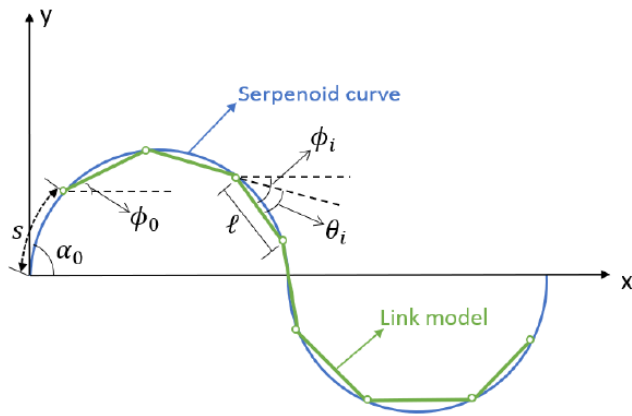


Fig. 16: Model of a serpenoid curve, shown in blue, and the segmented link model, shown in green, shows definitions of variables α_0 , s , l , ϕ , and θ . Figure adapted from [39].

The Overview of Snake Robot

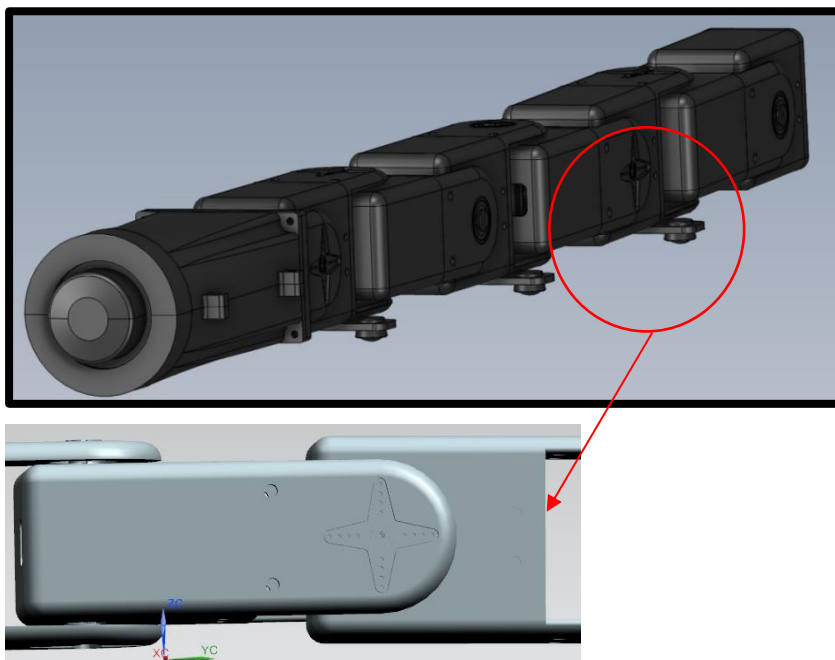


Fig. 18: The Final Rendered model of Snake Robot done in **SOLIDWORKS 2021**. The Snake robot consists in total 12 modules (Head + Tail) and the local magnification of a single module.

<u>Physical Units</u>	<u>Specifications</u>
Dimensions (mm)	Module 140.9x50x68.2 (mm) length (full 12 Module robot): 823.3 mm length (head link): 172.2 mm length (start link): 136.4 mm
Mass (kg)	Module: 0.18kg Full 12 Module robot: 2.75kg
Joint Limit (θ)	[0-180 degrees]
Used Material	PETG (Polyethylene Terephthalate Glycol)

Lateral Undulation:

True lateral undulation provides for a continuous sliding motion along the ground. The issue in the simulation is that the surface the robot moves along is flat; the ground plane could be populated with an array of small objects that the system could push against. This locomotion configuration also slightly lifts the outward lateral wave. This is the the ‘sinus lifting’ mentioned by Hirose.

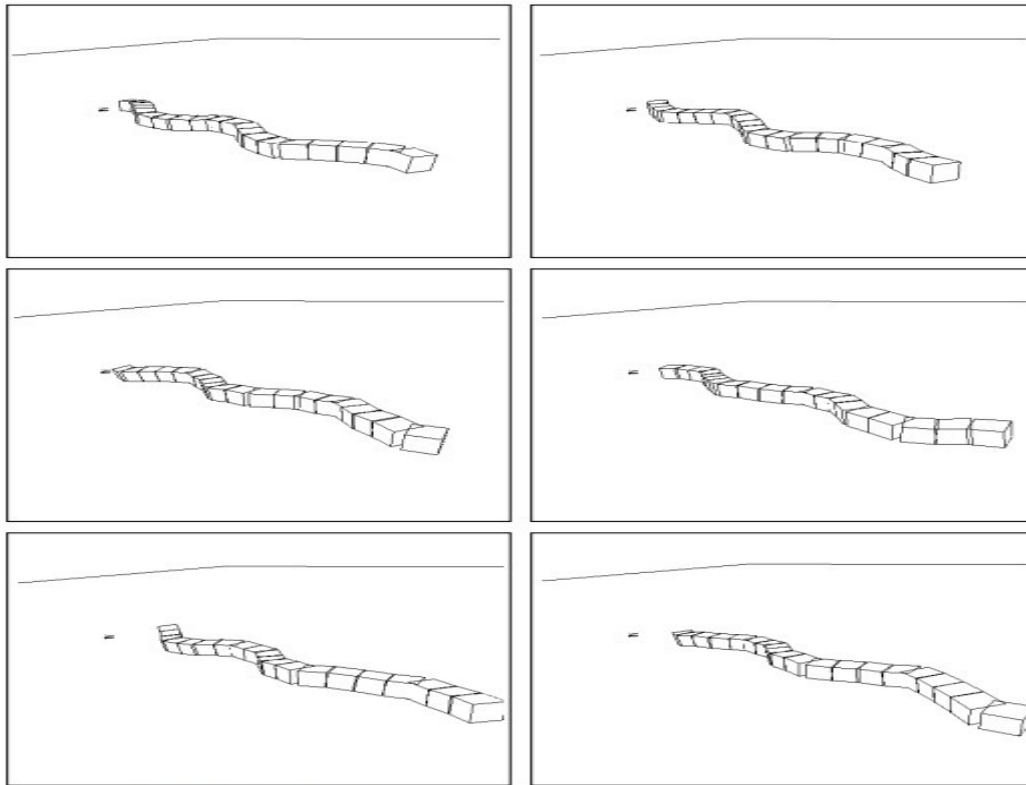


Figure 7-5: Lateral undulation.

Sidewinding Locomotion:

Sidewinding is a relatively efficient mode of locomotion with little sliding ground contact but with an odd means of moving laterally. Sidewinding is really two waves, one ventral and one lateral that are out of phase. Together they produce a motion that moves a body section to the side and the rest moves along and settles the body down to form successive parallel tracks as it moves.

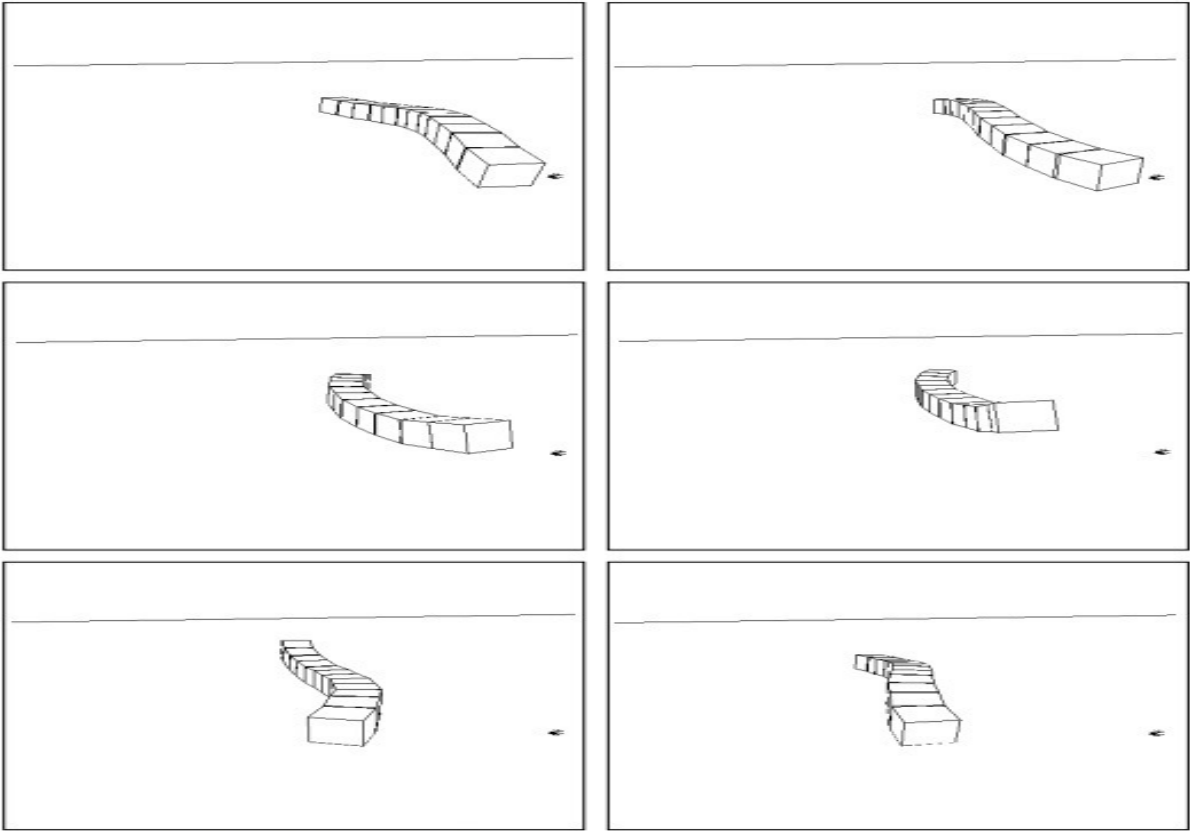


Figure 7-3: Sidewinding locomotion.

ELECTRONICS

The primary purpose of the electronics in the bot is to actuate the joints of the snake in such a manner that lateral undulation and sidewinding locomotion can be emulated. To this end, we make use of the following electronic components:

Components used:

1) TowerPro MG-996R:

- a) The MG-996R servo actuates the pitch and yaw joints of the snake robot so that snake motion can be emulated. The MG-996R has a torque of 11Kgf.cm at an operating voltage of 6V, allowing it to easily move the modules with power to spare.
- b) It has an operating temperature range of 0°C - 55°C, meaning it can function efficiently in a wide range of environments.
- c) Standing at 40.7 x 19.7 x 42.9 mm, it is small enough to fit in a compact snake design while also delivering enough torque to actuate the joints as required.



Fig. 19: TowerPro MG-996R Servo with included cabling.

2) LM-2596 DC-DC Converter:

- a) The LM-2596 functions as a buck converter, to step down the resultant voltage of 7.5V from the batteries to 6.5V to prevent the servos from getting damaged.
- b) It also delivers a constant supply of voltage to the servos to prevent the windings from getting damaged.



Fig. 20: Top view of an LM-2596 DC-DC converter.

3) FlySky - I6 Transmitter:

- a) FlySky - i6 transmitter functions as the remote control with which we give commands to the Arduino Nano through the FlySky - r6b receiver.
- b) It has six different radio channels to allow us a wide range of customisation with regards to the commands that can be provided.
- c) It has an inbuilt display to easily calibrate and customize the radio channels, update the firmware and show the amount of charge left in the batteries.



Fig. 21: An FS-I6 transmitter module out-of-the-box

4) FlySky - R6B Receiver:

- a) FlySky - R6B receiver module takes the commands sent by the FS - I6 transmitter and sends them to the Arduino Nano.

- b) It has a range of upto 2 Km, allowing for very long range control when coupled with the video and audio feed from the camera.
- c) It has an RF range of 2.405Hz - 2.475Hz with a bandwidth of 500 KHz, meaning it does not interfere with any other radio signals.



Fig. 22: Top view of FS-R6B receiver module

5) 18650 Battery Shield:

- a) The 18650 battery shield boosts the 3.7V output of the 18650 battery into 5V to supply to the Arduino Nano, R6B receiver and the V380 Camera.



Fig. 23: Image of 18650 Battery shield showcasing its multiple output options.

6) 3.7V/1950 mAH LiPo batteries:

- a) These batteries power the servo motors. We connect two 3.7V batteries in series to deliver 7.5V to the LM-2596 which steps it down to 6.5V.
- b) With a capacity of 1950 mAH, the batteries can easily power the servos for more than 90 minutes, with a theoretical maximum runtime of 2.1 hours (130 minutes).
- c) The batteries are rechargeable, meaning they can be reused.



Fig. 24: A standard 3.7V/1950mAh LiPo battery.

7) 18650 batteries:

- a) These batteries are used to power the Arduino Nano and the V380 camera.
- b) Their cylindrical shape means that they are the better choice for the head module, as their output can easily be boosted to the required 5V using the battery shield.
- c) They have a capacity of 2200 mAh, meaning they can power the Nano for 115 hours and the camera for 2 hours.



Fig. 25: A variant of the commonly used 18650 battery

8) Arduino Nano:

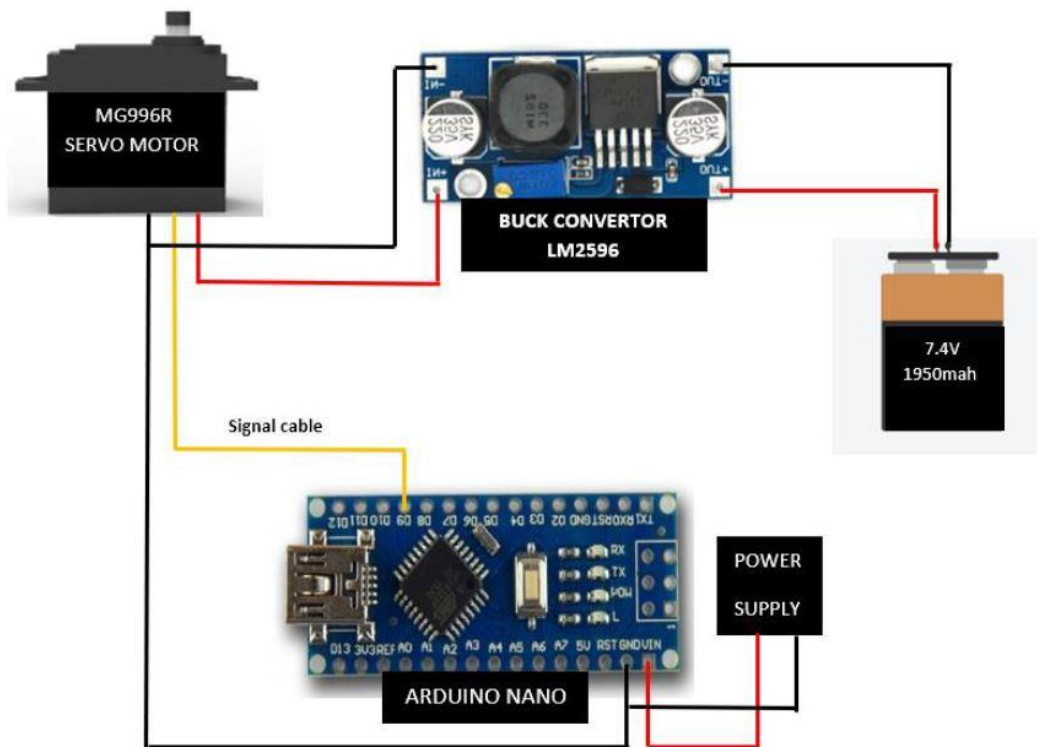
- a) The Nano is the primary processing unit of the bot, performing all the necessary computations to provide signal bits to the servo motors to replicate snake gaits at the joints of the snake.
- b) The Nano is powered by an ATmega 328, which has 32 KB Flash memory, 1 KB EEPROM and 2KB of SRAM which provides ample memory to write the code required.

- c) It has 22 digital and 8 analog pins which are more than sufficient to connect all the MG-996R servos and the FS-R6B receiver.
- d) It draws a measly 19mA of current, making it ideal for battery-driven applications such as this.

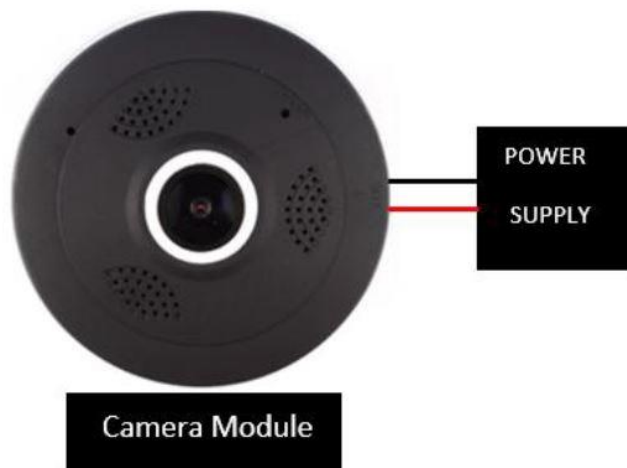


Fig. 26: Top view of Arduino Nano showcasing its pin layout.

Circuit Diagram:



Circuit diagram of a single segment connected to Master Arduino

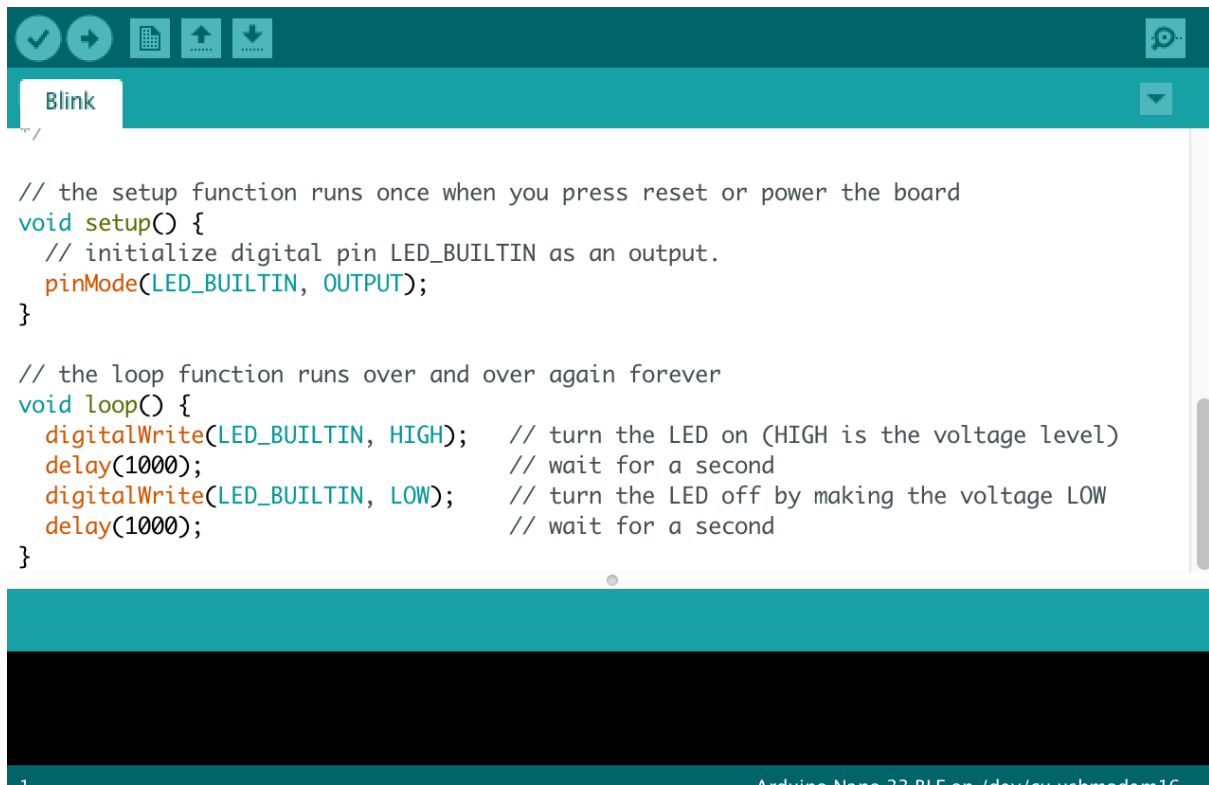


Camera Module with Power supply

Source Code

Software Used:

The only software we use throughout the project is the Arduino IDE, which is an open-source software that provides a GUI to write code for the Arduino board, as well as allows us to upload the code to the Arduino. It also provides a single platform to download and manage all the third-party libraries that a developer might use, with easy update and downgrade functionality.



```
// the setup function runs once when you press reset or power the board
void setup() {
  // initialize digital pin LED_BUILTIN as an output.
  pinMode(LED_BUILTIN, OUTPUT);
}

// the loop function runs over and over again forever
void loop() {
  digitalWrite(LED_BUILTIN, HIGH); // turn the LED on (HIGH is the voltage level)
  delay(1000); // wait for a second
  digitalWrite(LED_BUILTIN, LOW); // turn the LED off by making the voltage LOW
  delay(1000); // wait for a second
}
```

Fig. 27: Arduino IDE with code for the “blink” example.

Libraries Used:

We only make use of the Servo library, which allows us to control Servo motors using the PWM pins that are present on the Arduino Nano. No additional libraries are necessary.

Brief explanation:

Arduino code is written in a special version of C++, with additional libraries and functions. The Arduino IDE compiles and then translates this C++ code into machine language, allowing the ATmega 328 onboard to understand the commands supplied.

a) Lateral Undulation

```

for(int i=0; i<360; i++){
  rads=i*pi/180.0;
  for(int j=0; j<8; j+=2){
    myServos[j].write(90+offset+Amplitude*sin(Speed*rads+j*Wavelengths*Shift));
  }
  delay(10);
}
}

```

Fig.28: The primary logic behind lateral undulation

In order to achieve lateral undulation, we propagate a sine wave through all the laterally oriented, i.e, all the evenly numbered servos. The sine wave successfully replicates the zig-zag motion that snakes use in order to navigate from one point to another. Changing the offset variable allows us to change the direction of the snake, while the speed variable increases the rate of sine wave propagation allowing the snake to move faster.

b) Sidewinding Locomotion

```

for(int i=0; i<360; i++){
  rads=i*pi/180.0;
  for(int j=0; j<4; j++){
    myServos[2*j].write(90+offset+amplitude*sin(Speed*rads+j*Wavelengths*shift-(Multiplier-1)*pi/4));
    myServos[2*j+1].write(90+offset+amplitude*sin(Speed*rads+j*Wavelengths*shift+(Multiplier+1)*pi/4));
  }
  delay(10);
}
}

```

Fig.28: The primary logic behind sidewinding locomotion

Sidewinding locomotion can be achieved by passing a sine wave through the laterally oriented servos, and a cosine wave through the dorsally oriented servos. This creates a helical resultant motion, which closely mimics the sidewinding motion in which only two points of a snake are in contact with the ground.

Conclusions Drawn

- 1) The goal of this project is to investigate the locomotion mechanisms of multi-segmented and passively wheeled snake-like robots and characterize the robot's motion on varied sloped environments.
- 2) The snake-like robot is able to achieve serpentine locomotion by actuating the relative joint angles according to a simple mathematical description.
- 3) Successful reproduction of both lateral undulation and sidewinding locomotion has been achieved.
- 4) Sidewinding locomotion proves to be very effective to navigate over slippery terrain.
- 5) Analysis of the physical behaviours reveals that an incline will affect the motion by introducing an external gravitational force and reducing the maximum frictional force.

Future Work

The future work of this research is to collect more data on the motion characteristics of the snake robot on combined sloped environments or irregular terrain surfaces, so as to design advanced control strategies that allow the robot to track a position and velocity on a complex sloped environment and irregular terrains as well. As well as to aid in more superior combat operations, having tree climbing ability, Autonomous movement, Attaching Proximity Sensor & compact internal circuitry to the robot so that this snake robot can optimise and help the applications of it wherever applied.

Bibliography

- [1] G. Chirikjian and J. Burdick. The kinematics of hyper-redundant robot loco motion. *IEEE Transactions on Robotics and Automation*, 11(6):781–793, 1995. 1
- [2] S. Hirose. *Biologically Inspired Robots*. Oxford University Press, 1993. 1,2
- [3] B. Y. S. Hirose and H. Yamada. Snake-Like Robots. *IEEE Robotics & Automation Magazine*, (March):88–98, 2009. 1
- [4] H. Ohno and S. Hirose. Design of slim slime robot and its gait of locomotion. *Proceedings 2001 IEEE/RSJ International Conference on Intelligent Robots and Systems.*, pages 707–715, 2001. 1,2
- [5] M. Hara, S. Satomura, H. Fukushima, T. Kamegawa, H. Igarashi, and F. Matsuno. Control of a Snake-like Robot Using the Screw Drive Mechanism. *Proceedings 2007 IEEE International Conference on Robotics and Automation*, 28(3):541–554, Apr. 2007. 1
- [6] T. Kamegawa, T. Harada, and A. Gofuku. Realization of cylinder climbing locomotion with helical form by a snake robot with passive wheels. In *IEEE International Conference on Robotics and Automation (ICRA)*, pages 3067–3072, Kobe, Japan, 2009. 1
- [7] C. Wright, A. Buchan, B. Brown, J. Geist, M. Schwerin, D. Rollinson, M. Tesch, and H. Choset. Design and Architecture of the Unified Modular Snake Robot. In *IEEE International Conference on Robotics and Automation (ICRA)*, pages 4347–4354, St. Paul, USA, 2012. 1,2
- [8] C. Wright, A. Johnson, A. Peck, Z. McCord, A. Naaktgeboren, P. Gianfortoni, M. Gonzalez-Rivero, R. L. Hatton, and H. Choset. Design of a Modular Snake Robot. *Proceedings of the IEEE International Conference on Intelligent Robots and Systems*, Oct. 2007. 1
- [9] M. Yim, D. Duff, and K. Roufas. PolyBot: A Modular Reconfigurable Robot. In *IEEE International Conference on Robotics and Automation (ICRA)*, pages 514–520, San Francisco, USA, 2000. 1
- [10] M. Yim, W. Shen, and B. Salemi. Modular self-reconfigurable robot systems. *Robotics (March)*, 2007. 1
- [11] G. Chirikjian and J. Burdick. A modal approach to hyper-redundant manipulator kinematics. *IEEE Transactions on Robotics and Automation*, 10(3):343–354, June 1994. 1
- [12] J. Gonzalez-Gomez, H. Zhang, E. Boemo, and J. Zhang. Locomotion capabilities of a modular robot with eight pitch-yaw-connecting modules. In *9th international conference on climbing and walking robots*. Citeseer, 2006. 1

- [13] H. Ohno and S. Hirose. Design of slim slime robot and its gait of locomotion. Proceedings 2001 IEEE/RSJ International Conference on Intelligent Robots and Systems., pages 707–715, 2001. 1,2
- [14] S. Hirose. *Biologically Inspired Robots*. Oxford University Press, 1993. 1, 2
- [15] H. Yamada and S. Hirose. Approximations to continuous curves of Active Cord Mechanism made of arc-shaped joints or double joints. In IEEE International Conference on Robotics and Automation (ICRA), pages 703–708. IEEE, 2010. 1,2
- [16] H. Yamada and S. Hirose. Steering of pedal wave of a snake-like robot by superposition of curvatures. In IEEE/RSJ International Conference on Intelligent Robots and Systems (IROS), pages 419–424. IEEE, 2010. 1
- [17] J. Gonzalez-Gomez, H. Zhang, E. Boemo, and J. Zhang. Locomotion capabilities of a modular robot with eight pitch-yaw-connecting modules. In 9th international conference on climbing and walking robots. Citeseer, 2006. 1
- [18] A. Ijspeert and A. Crespi. Online trajectory generation in an amphibious snake robot using a lamprey-like central pattern generator model. In IEEE International Conference on Robotics and Automation (ICRA), pages 262–268. Ieee, Apr. 2007. 1
- [19] M. Tesch, K. Lipkin, I. Brown, R. L. Hatton, A. Peck, J. Rembisz, and H. Choset. Parameterized and Scripted Gaits for Modular Snake Robots. *Advanced Robotics*, 23(9):1131–1158, June 2009. 1,2
- [20] G. Chirikjian and J. Burdick. The kinematics of hyper-redundant robot locomotion. *IEEE Transactions on Robotics and Automation*, 11(6):781–793, 1995. 1
- [21] G. Chirikjian and J. Burdick. A modal approach to hyper-redundant manipulator kinematics. *IEEE Transactions on Robotics and Automation*, 10(3):343–354, June 1994. 1
- [22] A. A. Transth. *Modelling and Control of Snake Robots*. PhD thesis, Norwegian University of Science and Technology (NTNU), 2007. 1
- [23] A. A. Transth, K. Y. Pettersen, and P. I. Liljebäck. A survey on snake robot modeling and locomotion. *Robotica*, 27(07):999, Mar. 2009. 1
- [24] Gart SW, Mitchel TW, Li C. 2019 Snakes partition their body to traverse large steps stably. *J. Exp. Biol.* 59, jeb185991. (Doi:10.1242/jeb.185991)
- [25] Hu DL, Nirody J, Scott T, Shelley MJ. 2009 The mechanics of slithering locomotion. *Proc. Natl Acad. Sci. USA* 106, 10 081–10 085. (Doi:10.1073/pnas.0812533106)
- [26] Chirikjian GS, Burdick JW. 1995 The kinematics of hyper-redundant robot locomotion. *IEEE Trans. Robot. Autom.* 11, 781–793. (Doi:10.1109/70.478426)

- [26] Gatt SW, Mitchel TW, Li C. 2019 Snakes partition their body to traverse large steps stably. *J. Exp. Biol.* 59, jeb185991. (Doi:10.1242/jeb.185991)
- [27] Fr'ed'eric Boyer and AymanBelkhiri, "Reduced Locomotion Dynamics with Passive Internal DoFs: Application to Nonholonomic and Soft Robotics", *IEEE Transactions on Robotics*, vol. 30, no. 3, pp. 578-592, June 2014.
- [28] Fr'ed'eric Boyer, Shaukat Ali, and Mathieu Porez, "Macrocontinuous Dynamics for Hyperredundant Robots: Application to Kinematic Locomotion Bioinspired by Elongated Body Animals", vol. 28, no. 2, pp. 303-316, *IEEE Transactions on Robotics*, April 2012.
- [29] Aksel Andreas Transeth, Remco I. Leine, ChristophGlocker, Kristin Ytterstad Pettersen and P°alLiljeb"ack, "Snake Robot Obstacle-Aided Locomotion: Modeling, Simulations, and Experiments", *IEEE Transactions on Robotics*, vol. 24, no. 1, pp. 88-104, February 2008.
- [30] Rollinson, D.; Bilgen, Y.; Brown, B.; Enner, F.; Ford, S.; Layton, C.; Rembisz, J.; Schwerin, M.; Willig, A.; Velagapudi, P. Design and architecture of a series elastic snake robot. In *Proceedings of the IEEE/RSJ International Conference on Intelligent Robots & Systems*, Chicago, IL, USA, 14–18 September 2014.
- [31] Bing, Z.; Cheng, L.; Chen, G.; RaHrbein, F.; Huang, K.; Knoll, A. Towards autonomous locomotion: CPG-based control of smooth 3D slithering gait transition of a snake-like robot. *Bioinspire. Biomimetics* 2017, 12, 035001.
- [32] Melo, K. Modular snake robot velocity for side-winding gaits. In *Proceedings of the 2015 IEEE International Conference on Robotics and Automation (ICRA)*, Seattle, WA, USA, 26–30 May 2015; pp. 3716 3722.
- [33] Kajita, S.; Hirukawa, H.; Harada, K.; Yokoi, K. *Introduction to Humanoid Robotics*; Springer: Berlin, Germany, 2014; Volume 101.
- [34] Yamada, H.; Hirose, S. Approximations to continuous curves of Active Cord Mechanism made of arc-shaped joints or double joints. In *Proceedings of the IEEE International Conference on Robotics & Automation*, Anchorage, AK, USA, 3–7 May 2010.
- [35] Oprea, J. *Differential Geometry and Its Applications*; American Mathematical Soc.: Providence, RI, USA, 2019; Volume 59.
- [36] S. Hirose and H. Yamada, "Snake-like robots," *IEEE Robotics Automation Magazine*, vol. 16, no. 1, pp. 88–98, 2009.
- [37] S. Ma, N. Tadokoro, B. Li, and K. Inoue, "Analysis of creeping locomotion of a snake robot on a slope," *2003 IEEE International Conference on Robotics and Automation*, pp. 15–23.

- [38] S. Ma, "Analysis of creeping locomotion of a snake-like robot," *Advanced Robotics*, vol. 15, no. 2, pp. 205–224, 2001.
- [39] A. Saha, R. P. Chatterjee, and U. Dutta, "Motion control of snake robot by lead-lag compensator designed with frequency domain approach." *World Scientific and Engineering Academy and Society (WSEAS)*, 2009, pp. 13–20.
- [40] S. Ma, N. Tadokoro, B. Li, and K. Inoue, "Analysis of creeping locomotion of a snake robot on a slope," *2003 IEEE International Conference on Robotics and Automation*, pp. 15–23.